



## Research article

# Untreated plant waste of the Mediterranean region as bioadsorbent of persistent organic pollutants

Nicola Colatorti<sup>\*</sup>, Carlo Porfido, Danilo Vona, Giorgio Mazziotta, Elisabetta Loffredo

Dipartimento di Scienze del Suolo, della Pianta e degli Alimenti, Università degli Studi di Bari Aldo Moro, Via Amendola 165/A, 70126, Bari, Italy

## ARTICLE INFO

**Keywords:**

Orange peel  
Olive stone  
Pistachio shell  
SEM  
TXRF  
FTIR-ATR  
Adsorption  
Biowaste

## ABSTRACT

The excessive and/or improper use of plant protection products (PPPs) can generate alarming levels of residues in the environment, compromising both soil fertility and food safety. Various organic wastes released in large amounts by agro-industrial activity are currently studied and applied as bioadsorbents for water and soil decontamination. This study explored the capacity of untreated orange peel, olive stones and pistachio shells to adsorb the PPPs oxyfluorfen (OXY), metribuzin (MET) and imidacloprid (IMI), and the xenoestrogen bisphenol A (BPA) from water. The physicochemical, microstructural, and spectroscopic characteristics of the adsorbents were first evaluated using TXRF, SEM and FTIR-ATR techniques. Adsorption kinetics showed that each pollutant was rapidly (~24 h) retained by all adsorbents according to a pseudo-second order model, which suggested a prevalent chemisorption. Interpretation of the sorption isotherm data with various theoretical equations showed that all molecules on all adsorbents preferentially followed the Freundlich model. Among the materials, olive stones showed the highest adsorbent capacity with  $K_F$  values equal to 713, 317, 359 and 736  $\text{mg kg}^{-1}$  for OXY, MET, IMI, and BPA, respectively. The desorption of each compound from all materials was hysteretic. Based on the overall results obtained, it appears that all three materials tested may have interesting applications for the retention of organic pollutants, especially very hydrophobic ones. This paves the way for further investigations into natural adsorbents as sustainable tools for environmental remediation.

## 1. Introduction

In recent decades, intensive agricultural practices have not always complied with the recommended guidelines [1] for the use of plant protection products (PPPs), with harmful consequences of contaminating soil, ground- and surface water [2,3]. Repeated applications of PPPs and the accumulation of their residues in soil over the years can compromise not only soil fertility and crop productivity but also food quality and safety [4,5]. Among PPPs, herbicides and insecticides are largely employed to protect tree and herbaceous crops. Oxyfluorfen [2-chloro-1-(3-ethoxy-4-nitrophenoxy)-4-(trifluoromethyl) benzene] (OXY) is a diphenyl ether herbicide used to eliminate broadleaf weeds and acts by interrupting the final phase of chlorophyll synthesis [6]. Metribuzin [(4-amino-6-tert-butyl-3-(methylsulfanyl)-1,2,4-triazine-5(4H)-one] (MET) is a triazinone herbicide widely used in both pre- and

<sup>\*</sup> Corresponding author. Dipartimento di Scienze del Suolo, della Pianta e degli Alimenti, Università degli Studi di Bari Aldo Moro, Via Amendola 165/A, 70126 Bari, Italy.

E-mail address: [nicola.colatorti@uniba.it](mailto:nicola.colatorti@uniba.it) (N. Colatorti).

<https://doi.org/10.1016/j.heliyon.2024.e40740>

Received 27 June 2024; Received in revised form 15 October 2024; Accepted 26 November 2024

Available online 28 November 2024

2405-8440/© 2024 The Authors. Published by Elsevier Ltd. This is an open access article under the CC BY-NC-ND license (<http://creativecommons.org/licenses/by-nc-nd/4.0/>).

post-emergence to control broadleaf weeds, especially annual ones, in various crops [7]. Being a quite soluble molecule, MET has a great potential for leaching to groundwater [8]. Imidacloprid [1-((6-chlor-3-pyridinyl) methyl)-N-nitro-2-imidazolidinimine] (IMI) is one of the most used insecticides on a global scale and is currently suspected of exterminating pollinators and harming users [9]. This systemic neonicotinoid insecticide is employed in soil applications, directly on vegetation and to control pet parasites [10].

In addition to PPPs, endocrine disrupting chemicals (EDCs) can be released in soil by amendment practices that use not completely depolluted sludge and wastewater [11]. Among EDCs, bisphenol A [2,2-(4,4 dihydroxyphenyl) propane] (BPA) is one of the most widely produced chemical compounds in the world, with an estimated annual production of about 8 million tons [12]. BPA is a component of polycarbonate, epoxy resins, medical devices, paints, electrical and electronic components; it has a great relevance for its estrogenic and antiandrogenic effects [13].

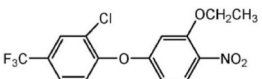
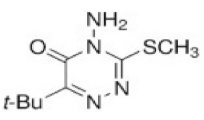
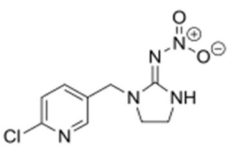
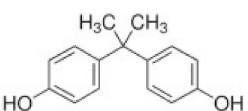
Both PPPs and EDCs often coexist in the soil and can be easily absorbed by plant roots and accumulated into edible plant parts, such as fruits, tubers, rhizomes, stems and flowers, thus entering the animal and human food chain [5,14].

The techniques currently used to remove organic pollutants from soil and wastewater include adsorption on organic and mineral matrices [15,16], membrane filtration systems [17], reverse osmosis [18], oxidation [19], ozone treatment [20] and photolysis [15]. Among these methods, the adsorption process is efficient, economical and environmentally friendly [21]. In the last years, bioenergy byproducts and derivatives, such as biochar, hydrochar, digestate and compost, are successfully employed for soil and wastewater remediation [16]. With a view to environmental and economic sustainability, recent research has focused on widely available agricultural waste and by-products to be used as bioadsorbents of organic and inorganic contaminants [22–24]. This nature-based and low-cost approach has a clear character of simplicity and effectiveness and is acclaimed by the population [25,26].

Three agro-industrial by-products that are particularly abundant in the Mediterranean area that could be used for bioremediation practices are orange peel, olive stones and pistachio shells. Orange is one of the most consumed fruits in the Mediterranean countries, with a global production exceeding 5 million tons in 2022 [27]. About 70 % of the citrus products are processed [28], and that generates large amounts of biowaste. The dominant components of orange peels are cellulose, hemicellulose, pectin, lignin, chlorophyll pigments and low molecular weight compounds [29]. Olive cultivation occupies about 5 million hectares of the Mediterranean area [30] and the disposal of waste from the olive oil industry (including olive stones) is a worrying environmental issue, especially in major producing countries such as Spain and Italy [31,32]. In recent years, the pistachio fruit has had growing appreciation by consumers and the agri-food industry, reaching a global production of 1 million tons in 2022 [33], of which the shells accounts for 15 % of the product [34]. The olive stones and the pistachio shells are similar in lignin, cellulose, and hemicellulose contents [35,36].

These by-products have been used so far mostly as fuels, with consequent loss of C in the atmosphere and release of air-pollutants (carbon monoxide, nitrogen oxides, and particulates such as soot and ash from combustion) [37,38]. Another current use of the three by-products is the thermochemical and biological treatment to produce bioenergy and C-rich solid residues, such as biochar, digestate and compost [34,39,40], which contributes to carbon sequestration strategies aimed at mitigating climate change [41,42]. Biochar, digestate and compost have shown excellent capacity in the retention of both organic and inorganic pollutants [43–45]: as such, they are often applied for soil restoration. In this context, biochar and activated carbon are particularly interesting because of their high surface area, long term stability and high carbon content [46,47]. However, the thermochemical conversion of biomass, requires large energy inputs, posing questions from the point of view of economic and environmental sustainability [48]. Furthermore, the efficiency of the biochemical conversion of waste, such as composting and anaerobic digestion, is strictly related to the feedstock; biowastes such

**Table 1**  
Some properties of the compounds.

Compound	Chemical structure	Molecular weight (g mol <sup>-1</sup> )	Water solubility at 25 °C (mg L <sup>-1</sup> )	log Kow
Oxyfluorfen		361.70	~2	4.73
Metribuzin		214.29	1200	1.70
Imidacloprid		255.70	610	0.57
Bisphenol A		228.29	300	3.32

Data from PubChem open chemistry database at the National Institutes of Health (2024).

as olive stones and pistachio shells are not the most suitable due to the high lignin content and the resulting high C/N ratio [35,36]. Differently, the direct use of untreated wastes does not require energy-intensive processing and specialized equipment, and can represent an effective and economic alternative due to the low cost, wide availability and a chemical structure suitable for the retention of contaminants [49,50]. To the best of our knowledge, these materials have never been tested as adsorbents of organic contaminants [51].

In light of the above, the main objective of this study was to assess the effectiveness of three agro-industrial by-products, orange peel, olive stones and pistachio shells, to act as natural adsorbents of some chemicals, namely OXY, MET, IMI and BPA, from water. Quantitative data were obtained from adsorption kinetics and adsorption/desorption isotherms. Furthermore, to relate the sorption capacity of these materials to their properties and structure, a preliminary extensive characterization was carried out using total reflection X-ray fluorescence (TXRF) spectroscopy, scanning electron microscopy (SEM) analysis and Fourier transform infrared (FTIR) spectroscopy.

## 2. Materials and methods

### 2.1. Chemicals and adsorbents

The four molecules OXY, MET, IMI and BPA at purities of 99.0, 98.0, 99.0 and 99.0 %, respectively, were purchased from Sigma-Aldrich S.r.l, Milano, Italy. Structural formula and some chemical properties of the compounds are reported in Table 1. All other chemicals of extra pure grade were obtained from commercial sources and used without further purification.

Adsorbents obtained from orange peel, olive stones and pistachio shells were used. The orange peel was collected from 'Navelina' orange (*Citrus sinensis* L.), a variety for fresh consumption, purchased at the local market. The olive stones were supplied by the cooperative 'Il Sannicandrese', Sannicandro di Bari, Italy, while the pistachio shells were of domestic origin. Before experiments, the materials were repeatedly washed with tap water, soaked in deionized water for approximately 1 h to remove residual impurities, dried at a temperature of 40 °C for 36 h and finally ground to < 1-mm particles.

### 2.2. Adsorbent characterization

#### 2.2.1. Basic characterization

Physicochemical characterization of the three adsorbents was carried out according to conventional methods. Moisture was measured after heating the adsorbents at 105 °C overnight. Bulk density (BD) was measured using a 500 mL graduated cylinder filled with a known sample mass and tapped manually for 60 s to ensure the absence of large void spaces, before measuring the final volume occupied by the sample mass. The ash content was determined after drying the samples in a muffle furnace at the temperature of 550 °C for 4 h. The pH and EC were measured using a pH meter and a conductivity meter (adsorbent/H<sub>2</sub>O, 1:10, w/v), respectively. Total organic matter was determined by the loss on ignition method [52].

#### 2.2.2. Elemental analysis

Minor and trace elements present in the three adsorbents were analysed by TXRF spectroscopy using a S2 Picofox Spectrometer (Bruker Nano GmbH, Berlin, Germany). The instrument was equipped with a Mo microfocus tube (30 W, 50 kV, 600 µA), a multilayer monochromator, and an XFlash® silicon drift detector with a 30 mm<sup>2</sup> active area. The energy resolution, measured at the K $\alpha$  of Mn, was <150 eV (10 keps). For such analysis, dried samples were finely powdered using a vibratory ball mill (model MM200, Retsch) for 5 min. Then, for each sample, 10 mg of powder were suspended in 3 mL of Triton X-100 (1:100, v/v in bidistilled water) using 10 mL plastic tubes and left for 10 min in an ultrasonic bath. After that, 10 mL of a 1000 mg L<sup>-1</sup> Y standard (Sigma-Aldrich) were added to each suspension as internal standard. Finally, after vortexing for 30 s, 10 µL of suspension were pipetted onto siliconized quartz carriers and left until complete dryness on a heating plate (50 °C) under a laminar flow hood. All samples were analysed in triplicate for 1000 s, and the results were obtained with the software Spectra 7 (Bruker GmbH, Germany).

#### 2.2.3. SEM analysis

SEM analysis was performed to investigate the surface micromorphology of the adsorbents. The sample was fixed with an adhesive carbon tape, metallized with Au, and analysed with a high-resolution field emission scanning electron microscope VP FE-SEM SIGMA 300 (ZEISS, Oberkochen, Germany). The SEM micrographs of the three adsorbents were captured at 1500× magnifications using a 5 kV acceleration potential.

#### 2.2.4. FTIR-ATR spectroscopy

FTIR spectroscopy coupled with attenuated total reflectance (ATR) was used to investigate functional groups belonging to the chemical bulks of the three materials. A PerkinElmer Two Spectrophotometer equipped with A 2 × 2 mm diamond crystal was exploited. After fine pot milling 0.2 g of each dried sample, 2.5-mg sub-samples were spread over diamond surface and analysed (4000-400 cm<sup>-1</sup> range, 4 cm<sup>-1</sup> resolution, 32 scan, 2 cm s<sup>-1</sup> rate). Each recorded scan set was averaged, corrected against ambient air as background and treated with ATR correction correlative function. To highlight the emerging bands, the smoothing function of the workstation was not needed.

### 2.3. Adsorption kinetics

An adsorption kinetics study was conducted in batch mode to quantify the adsorption of OXY, MET, IMI and BPA on the three adsorbents and to estimate the time needed to reach the adsorption equilibrium. Aliquots of 10 mg of adsorbents were interacted with 20 mL of an aqueous solution (solution/adsorbent ratio equal to 2000) of the four molecules, each at a concentration of 2 mg L<sup>-1</sup>, in glass centrifuge tubes. The suspensions were stirred for 0.017, 0.083, 0.17, 0.25, 0.5, 1, 4, 16 and 24 h in the dark at 310 rpm and 20 ± 1 °C. After each time, the suspensions were centrifuged at 10,000 g for 10 min at 10 °C. The equilibrium concentration of each compound in the supernatant solution was determined by ultra-high performance liquid chromatography (UHPLC) as described in section 2.5. All experiments were performed in triplicate.

The amount of each compound adsorbed on the adsorbent at each time *t*, *q<sub>t</sub>* (mg kg<sup>-1</sup>), was calculated by the equation  $q_t = (C_0 - C_t) V/m$ , where *C<sub>0</sub>* (mg L<sup>-1</sup>) is the initial concentration of the compound in solution, *C<sub>t</sub>* (mg L<sup>-1</sup>) is the concentration of the compound at time *t*, *V* (mL) is the volume of the solution and *m* (g) is the mass of the adsorbent. The equilibrium time was established when at two successive times the quantity of compound adsorbed was unchanged according to the Student's *t*-test (*p* ≤ 0.05).

### 2.4. Adsorption and desorption isotherms

Adsorption isotherms were studied to quantitatively evaluate the adsorption of the four molecules on the adsorbents and obtain the values of the adsorption parameters. Volumes of 20 mL of an aqueous solution of the molecules, each at concentrations of 0.1, 0.2, 0.5, 1 and 2 mg L<sup>-1</sup>, were added to aliquots of 10 mg of adsorbent in glass centrifuge tubes. The samples were stirred for 24 h in the dark at 20 ± 1 °C to achieve the steady state. Subsequently, the suspensions were centrifuged at 10,000 g for 10 min at 10 °C. The equilibrium concentration of the compounds was determined using UHPLC as described in the next section.

Desorption experiments were started immediately after adsorption, adopting the samples added with the molecules at 2 mg L<sup>-1</sup>. At each of the three subsequent desorption steps, a volume of 16 mL of supernatant solution was replaced with the same volume of double distilled water. The samples were stirred again for 24 h at 20 ± 1 °C and centrifuged in the conditions reported above. The solution concentration of the compounds at each desorption step was measured using UHPLC (see next section). All adsorption and desorption experiments were triplicated.

### 2.5. Chromatographic analysis

The four compounds were quantified by an UHPLC apparatus (Dionex Ultimate 3000 RSLC, Waltham, MA, USA) equipped with an HPG-3200 RS pump, a WPS-3000 automatic sampler, and a TCC-3000 column compartment connected to a Supelco™ LC-18 column (250 mm × 4.6 mm × 5 μm). The mobile phase was a mixture of water (A) and acetonitrile (B) flowing at 0.8 mL min<sup>-1</sup>. The elution gradient was: 0–1 min, 60 % A; 1–4 min from 60 to 40 % A; 4–8 min, from 40 % to 30 % A; 8–12 min, from 30 to 10 % A. The retention times of OXY, MET, IMI and BPA were 4.8, 3.5, 1.8, and 7.6 min, respectively. The compound OXY, MET and IMI were detected using a diode series detector DAD-3000 RS (Dionex Ultimate 3000 RSLC, Waltham MA, USA) at wavelengths of 210, 294 and 269 nm, respectively, while BPA was quantified using a FLD-3400 RS (Dionex Ultimate 3000 RSLC, Waltham, MA, USA) fluorescence detector operating at wavelengths of 230 and 310 nm for excitation and emission, respectively.

### 2.6. Theoretical equations

To investigate the adsorption mechanism, experimental kinetics data were interpreted with the pseudo-first order (PFO) [53] and pseudo-second order (PSO) [54] models. The non-linear form of the pseudo-first order equation is expressed as:  $q_t = q_e (1 - \exp^{-k_1 t})$ , where *q<sub>e</sub>* and *q<sub>t</sub>* are the amount of solute adsorbed per mass unit of adsorbent (mg kg<sup>-1</sup>) at equilibrium and at time *t*, respectively, and *k<sub>1</sub>* (h<sup>-1</sup>) is the PFO adsorption constant. The non-linear regression was used to obtain *q<sub>e</sub>* and *k<sub>1</sub>* values. The non-linear form of the PSO equation is:  $q_t = \frac{q_e^2 k_2 t}{1 + k_2 q_e t}$ , where *q<sub>e</sub>* and *q<sub>t</sub>* were already described and *k<sub>2</sub>* (kg mg<sup>-1</sup> h<sup>-1</sup>) is the PSO constant. Also for this equation, the non-linear regression was adopted to calculate the values of the parameters *q<sub>e</sub>* and *k<sub>2</sub>*.

Adsorption and desorption isotherms data were interpreted with the Henry, Freundlich and Langmuir equations. The linear model of Henry is given by:  $q_e = K_d C_e$ , where *q<sub>e</sub>* is the amount of compound adsorbed per unit of substrate (mg kg<sup>-1</sup>) at equilibrium, *C<sub>e</sub>* is the equilibrium concentration of the solute in solution (mg L<sup>-1</sup>) and *K<sub>d</sub>* is the distribution coefficient. The Freundlich equation is expressed as:  $q_e = K_f C_e^{1/n}$ , where 1/*n* indicates the degree of non-linearity between the solute concentration in solution and on the adsorbed, while *q<sub>e</sub>* and *C<sub>e</sub>* have the meaning already mentioned above. The Freundlich constants, *K<sub>F</sub>* and *n* indicate, respectively, the capacity and the intensity of adsorption. The Langmuir equation is given by:  $q_e = (K_L C_e b) / (1 + K_L C_e)$ , where *q<sub>e</sub>* and *C<sub>e</sub>* were defined previously, *b* represents the maximum adsorption capacity (mg kg<sup>-1</sup>) and *K* expresses the adsorption energy (L mg<sup>-1</sup>). The Freundlich (*K<sub>F</sub>* and 1/*n*) and Langmuir (*b* and *K<sub>L</sub>*) parameters were calculated using the non-linear regression method.

### 3. Results and discussion

#### 3.1. Characterization of adsorbents

##### 3.1.1. Basic characterization and elemental analysis

Basic properties of orange peel, olive stones and pistachio shells are reported in Table 2. All adsorbents showed an acidic pH, which is typical of these matrices [55,56]. The latter property suggests the suitability of these adsorbents in alkaline soils which are quite common in the Mediterranean region. EC values followed the order olive stones < orange peel < pistachio shells. As expected, the organic matter content of each adsorbent was very high (Table 2).

Several studies in the scientific literature report the compositional profile of such materials in terms of cellulose, hemicellulose, and lignin contents, which generally range as a whole within values of 80–99 % (dw) for olive stones [57] and 70–87 % (dw) for pistachio shells [58,59]. Gained [60] reported a total content of 98.9 % for orange peels. Furthermore, in these studies, the analysis of the chemical composition is generally limited to the major elements, such as C, H, N, O and S, since they influence the performance in their thermal conversion, such as combustion, which is currently their most common destination [57]. In contrast, less attention has been paid to minor and trace elements of these matrices (including hazardous metals), with very little published data. Indeed, while it is considered of primary importance to measure the concentration of elements such as Cr, Sr, Ni, Cu and so on in the edible parts of nuts [61], the metal load of shells and stones is generally neglected. However, for the purpose of this work, the inorganic content of these plant parts is of interest since, once incorporated into the soil, they could be a beneficial supply of plant nutrients but also a source of potentially toxic elements. For such a purpose, TXRF analysis was performed to evaluate qualitatively and quantitatively several major, minor and trace elements, namely P, S, K, Ca, Ti, Cr, Mn, Fe, Ni, Cu, Zn, Br, Rb, Sr and Pb, in each adsorbent (Table 3 and Fig. 1).

Among the major elements, P concentration was similar for all the three adsorbents, ranging from 0.12 to 0.14 %, while K content was significantly higher in orange peel compared to the other adsorbents. The P and K concentrations detected in orange peel (1212 and 5582 mg kg<sup>-1</sup>, respectively) are in accordance with what was found by Gained [60], who measured in orange peel 0.1 and 0.75 % of P and K, respectively. The S element was higher in pistachio shells than in orange peel and below the limit of detection in olive stones. The Ca content was similar in olive stones and pistachio shells (~0.1 %) and much higher in orange peel. Both in olive stones and pistachio shells, Ca and K concentrations were similar to those reported in the literature for these materials [59,62].

Regarding trace elements, pistachio shells showed the highest concentrations of Fe (100 mg kg<sup>-1</sup>) and Cu (64 mg kg<sup>-1</sup>); these values, although of the same order of magnitude, were quite different from those reported by Celik et al. [59] for Fe (420 mg kg<sup>-1</sup>) and Cu (5.3 mg kg<sup>-1</sup>). However, both the plant variety and the characteristics of the local soil can markedly influence the uptake and accumulation of these elements in the fruits and therefore in the shells [61,63]. Besides, the higher Fe content of pistachio shells with respect to the other bioadsorbents under investigation could be related to shells' intrinsic physiological function: indeed, in pistachio, as for other nuts, the primary role of the stony pericarp (i.e., the shell) is to surround and protect the inner kernel. Indeed, in this regard, it has been observed that an increase of heavy metal content in shells is correlated to an improvement of their physico-mechanical characteristics, such as density and tensile strength [59]. Differently from pistachio shells, Ti was below the instrumental limit of quantification (LOQ) in the other two adsorbents. The lowest Fe and Cu contents were found in orange peel (23 and 4 mg kg<sup>-1</sup>, respectively). All other elements detected never exceeded some units of mg kg<sup>-1</sup>, with the only exception of Sr (39.2 mg kg<sup>-1</sup>) in orange peel (Table 3). The content of the potentially toxic Pb was approximately 2 mg kg<sup>-1</sup> in each sample, while Zn concentration followed the order: olive stones < orange peel < pistachio shells, accounting for 8.6, 4.0 and 2.5 mg kg<sup>-1</sup>, respectively.

In light of the overall results of TXRF analysis, we can conclude that the incorporation of these materials into the soil, in addition to be an organic supply useful for the immobilization of contaminants, can provide important elements for plant nutrition (P, K, S, Fe and so on) without the risk of adding potentially toxic elements, which might happen with organic amendments derived from technological processes [64].

##### 3.1.2. SEM analysis

The SEM analysis is a useful tool to morphologically characterize complex organic matrices such as plant parts.

Images of the three adsorbents obtained at × 1500 magnifications are shown in Fig. 2. A heterogeneous surface, irregular structures, niches along with pores of different sizes and shapes were observed in all adsorbents. These features can favour the adsorption of pollutants on both the outer and inner parts of the adsorbents.

**Table 2**  
Some properties of the adsorbents.

Parameter	Orange peel	Olive stones	Pistachio shells
pH <sup>a</sup>	4.94 ± 0.10 <sup>b</sup>	5.27 ± 0.02	4.95 ± 0.11
EC <sup>a</sup> (dS m <sup>-1</sup> )	1.10 ± 0.01	0.19 ± 0.01	2.01 ± 0.04
Moisture (%)	9.50 ± 0.25	10.24 ± 0.38	6.46 ± 0.55
Ash (%)	2.97	0.54	3.20
BD (g cm <sup>-3</sup> )	0.49	0.53	0.53
Organic matter (% dw)	97.05 ± 0.06	99.35 ± 0.21	96.81 ± 0.24

<sup>a</sup> adsorbent/double distilled H<sub>2</sub>O 1:10 (w/v).

<sup>b</sup> SD (n = 3).

**Table 3**  
TXRF elemental analysis of the three adsorbents.

Element	Orange peel (mg kg <sup>-1</sup> dw)	Olive stones	Pistachio shells
P	1211.9 ± 85.2 <sup>a</sup>	1402.3 ± 56.4	1223.7 ± 28.4
S	162.3 ± 32.7	<LOQ	249.4 ± 8.5
K	5581.8 ± 228.1	1041.3 ± 36.1	2003.5 ± 117.6
Ca	5231.7 ± 336.6	1140.9 ± 104.4	905.3 ± 16.8
Ti	< LOQ	< LOQ	3.6 ± 0.3
Cr	< LOQ	< LOQ	10.3 ± 1.7
Mn	4.7 ± 0.7	4.8 ± 0.1	4.2 ± 0.2
Fe	22.8 ± 1.7	67.0 ± 8.3	99.9 ± 2.9
Ni	< LOQ	2.1 ± 0.3	5.6 ± 0.4
Cu	4.1 ± 0.3	6.0 ± 0.0	64.4 ± 8.4
Zn	4.0 ± 0.3	2.5 ± 0.2	8.6 ± 1.1
Br	3.7 ± 0.3	1.5 ± 0.2	4.0 ± 0.2
Rb	2.6 ± 0.3	1.5 ± 0.5	2.5 ± 0.2
Sr	39.2 ± 1.0	< LOQ	2.8 ± 0.2
Pb	2.3 ± 0.4	1.9 ± 0.4	1.8 ± 0.1

<sup>a</sup> Standard error (n = 3).

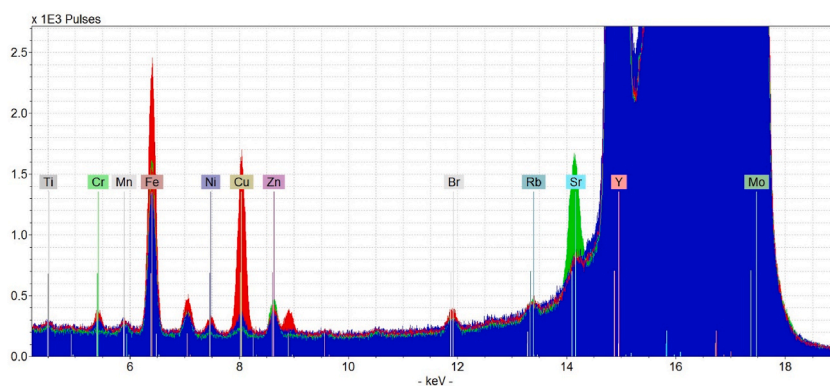


**Fig. 1.** Selected region of TXRF spectra of orange peel (green spectrum), olive stones (blue spectrum) and pistachio shells (red spectrum) showing some trace elements peaks. The Y peak (14.958 keV) and the Mo signals are attributable to the internal standard, and the Mo Compton and Rayleigh scattering, respectively.

### 3.1.3. FTIR-ATR analysis

Infrared investigations often offer advantages in characterization of complex biomasses, such as avoiding differential and detrimental treatment of the sample, the lack of the use of secondary reactions for derivatization, and the use of simultaneous measurements to speed up the investigation and related comparison. The Fourier-transform infrared (FTIR) spectroscopy was used here to focus and light on the presence of biomacromolecular functional groups found in orange peels, olive stones and pistachio shells. By a direct FTIR-ATR characterization of the orange peel biomass (Fig. 3a), significant signals set at  $\nu = 3297.2$  (-OH from carbohydrates of cellulose, water), 2915.0, 2855.0 (-CH S signal, symmetric, asymmetric peaked aliphatic chains, terpenoids), 2344.2–1985.3 aromatic overtones (W signal), 1742.3 (-C=O stretching, carboxyl), 1656.2 (-C=C- stretching), 1490.1, 1421.7 (-CH bending vibr.), 1013.2 (C–O–H or C–O–R from ester moieties and saccharides), 979.0, 879.0, 587.63 (finger print) were found. Signals are so ascribable to fatty acid esters, terpenoids and cellulose-like matrix moieties typical of this composite, and in line with literature [65,66]. The FTIR-ATR spectra of olive stones and pistachio shells (Fig. 3b and c) appeared very different from orange peel, although they were both almost overlapping. After recording spectra, the 1737 cm<sup>-1</sup> peak sets for C=O of carboxylic acids, while 1641–1580 peaked signals can be mostly attributed to C=O stretching and N–H bending of amide moieties and the fully enriched presence of peaks from 1590 to 1460 cm<sup>-1</sup> are due to C=C moiety found in aromatic lignolic/lignin-like compounds [67]. The related spectra report signals at 1240–1250 cm<sup>-1</sup> likely attributed to the stretching C–O moiety of the guaiacyl ring, while 900–894 cm<sup>-1</sup> signals can be attributed to the syringyl residue [68]. As reported in the literature [69], shells of dried fruits contain high level of hemicellulose (C–O–C of glycosidic link, around 1200–1050 cm<sup>-1</sup>) [70].

Under a biosorption and remediation point of view, and with an attempted focus on the molecular bases, cellulose macrostructures could in principle give direct interaction exploiting the polar -C–O and O–H functional groups with metal and charged organic pollutants. This dipole:ion and dipole:dipole interactions, with cumulative nature, are often dependent on the rate of humidity and the chemical environment surrounding or standing remediation process, while less affected by pH variations. -COOH and -NH<sub>2</sub> moieties are more switchable functional groups, often belonging to glycoconjugate and complex organic carboxyl acids, and natural

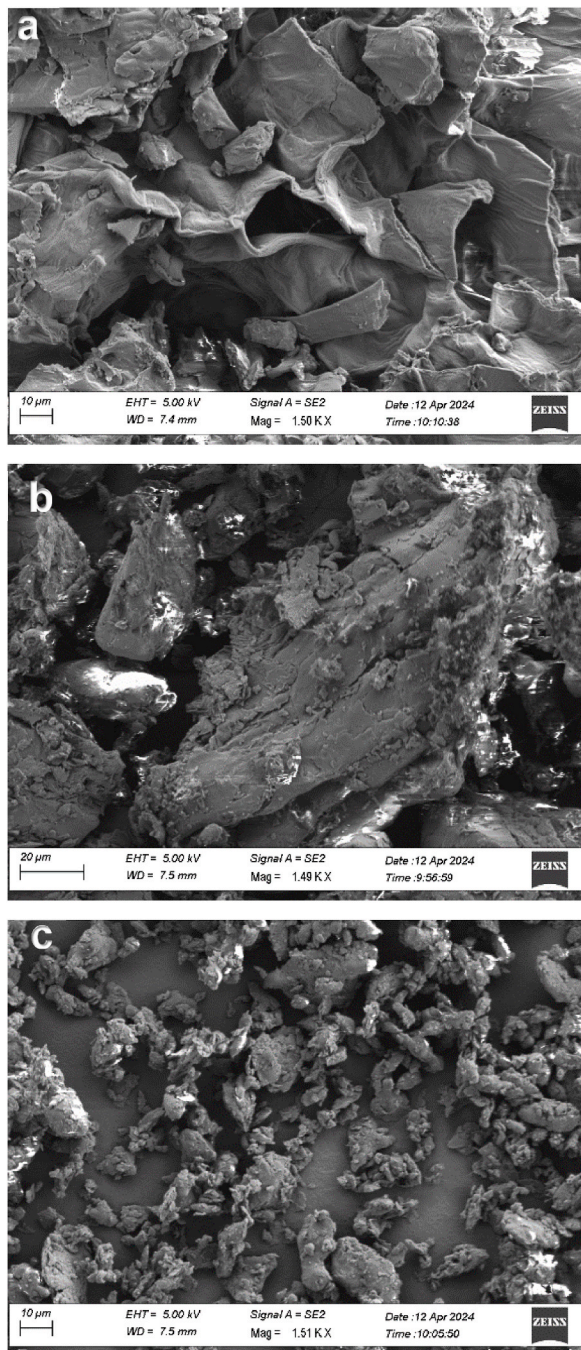
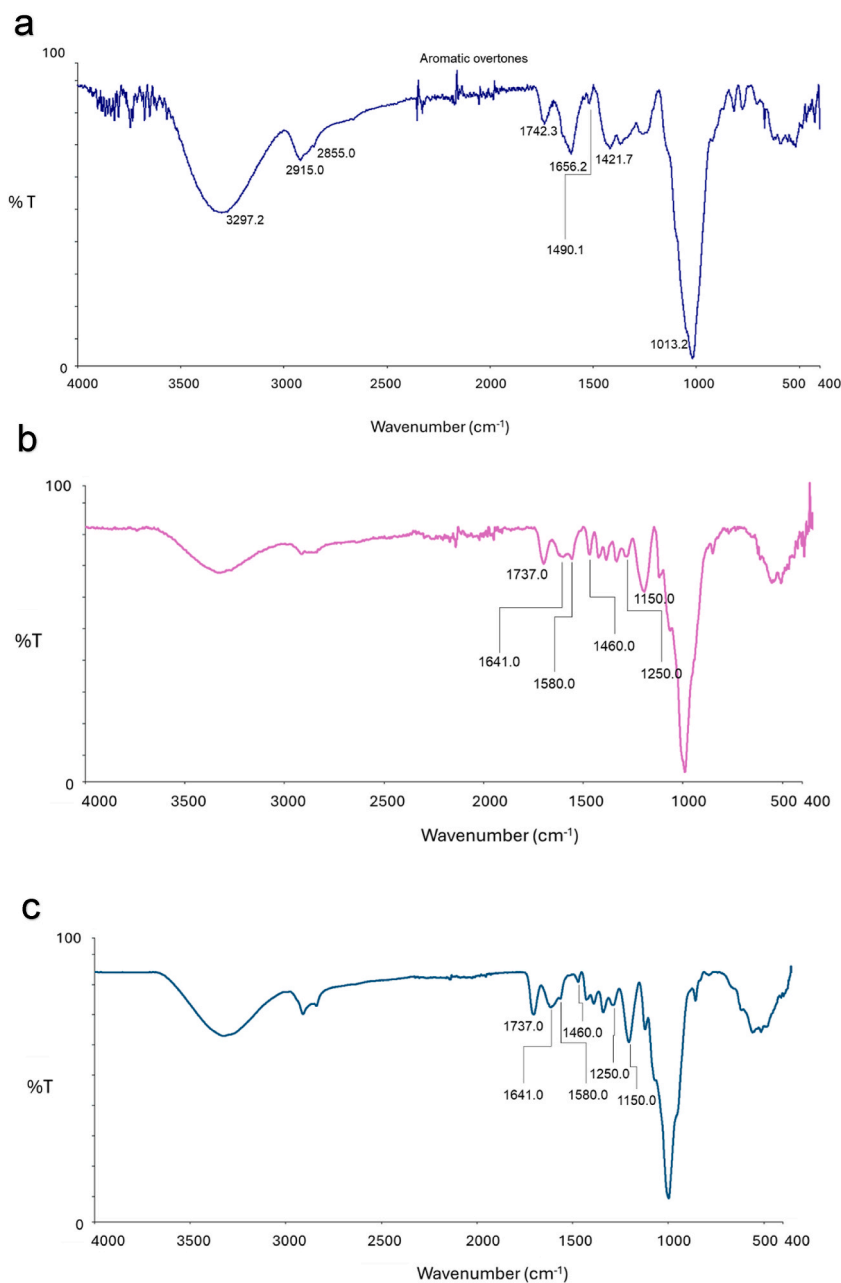


Fig. 2. Scanning electron microscopy (SEM) images at  $\times 1500$  magnifications of orange peel (a), olive stones (b), and pistachio shells (c).



**Fig. 3.** FTIR-ATR spectra of orange peel (a), olive stones (b), and pistachio shells (c).

polyamines. Varying pH values the buffering solution effect becomes so important, facilitating dipole:ion and ion:ion interaction at the matrix bulk or surface. In all these adsorbents, the presence of OH-enriched cellulosic moieties and the abundance of  $\pi$ - $\pi$  stacked aromatic structures with a certain degree of oxidation induced us to think this bulk chemistry as ideally exploitable to surface catch organic polar pollutants aiming to cheap bioremediation applications. In details, poly-hydroxy-indoles, oxidized catechols and lignin-based macrostructures allow a certain hetero  $\pi$ - $\pi$  stacking with the aromatic mono- and bi- or poly-nuclear aromatic pollutants [71], and these interactions strongly depend on the effective distance between pollutants and the matrix, the time of exposure, and the presence of different ligand-like interfering chemical species. All these functional groups, specifically all bio- and nature-based, are extraordinary because they can act combinatorially in the same matrix, and this property is rarely exhibited by artificial, industrial and pre-formed composites reported in literature, silica nanotubes, nanoparticles, nanorods, magnetic metal:organic frameworks, metal:zeolite composites [72].



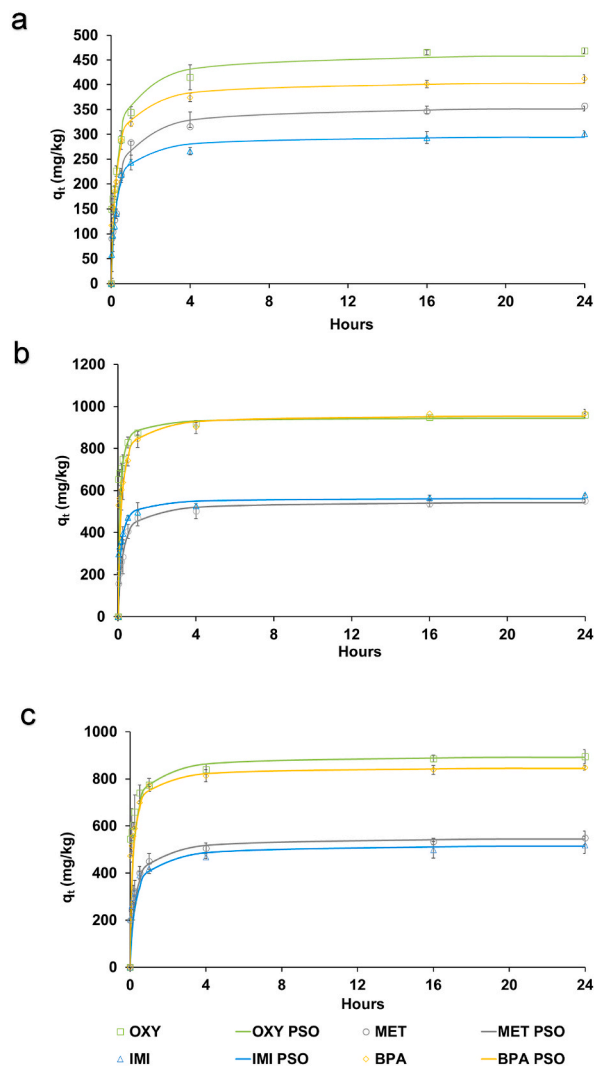


Fig. 4. Adsorption kinetics data and plots of predicted pseudo-second order (PSO) kinetics of OXY, MET, IMI and BPA onto orange peels (a), olive stones (b), and pistachio shells (c). Standard error is reported as vertical bar on each point ( $n = 3$ ).

**Table 4**  
Kinetic PFO and PSO parameters for the adsorption of the compounds on the adsorbents.

Adsorbent	Compound	PFO model					PSO model			
		$q_{e, exp}$	$r$	SSR	$q_{e,1}$ (mg g <sup>-1</sup> )	$k_1$ (h <sup>-1</sup> )	$r$	SSR	$q_{e2}$ (mg g <sup>-1</sup> )	$k_2$ (kg mg <sup>-1</sup> h <sup>-1</sup> )
Orange peels	OXY	468.8	0.951	5870	440.83	2.19	0.990	861	463.80	0.007
	MET	357.5	0.985	1079	338.59	2.02	0.991	602	356.68	0.008
	IMI	301.4	0.966	1234	283.22	2.70	0.979	699	297.38	0.014
	BPA	412.1	0.961	2760	387.82	2.63	0.981	418	407.12	0.010
Olive stones	OXY	959.0	0.847	7322	1327.34	1.09	0.999	600	960.96	0.009
	MET	551.3	0.845	2321	1305.92	1.02	0.999	1173	553.70	0.007
	IMI	579.9	0.839	4612	1316.66	1.09	0.999	1043	581.18	0.008
	BPA	967.8	0.874	14270	2040.19	1.13	0.999	1458	975.03	0.006
Pistachio shells	OXY	894.5	0.852	12113	1674.61	1.10	0.999	2102	898.32	0.007
	MET	549.2	0.840	4992	1542.13	1.09	0.999	410	550.92	0.007
	IMI	519.1	0.834	5301	1465.22	1.08	0.999	994	519.12	0.007
	BPA	847.8	0.847	4839	1380.27	1.09	0.999	260	849.93	0.009

### 3.2. Adsorption kinetics

The study of adsorption kinetics allows to quantitatively evaluate the retention of compounds present in solution on solid matrices and to establish the equilibrium time of the process. This study also provides information on the type of interaction between the adsorbent and the solute. Based on the adsorption kinetic curves, each molecule reached the adsorption equilibrium in a relatively short time (Fig. 4). The Student's t-test ( $P \leq 0.05$ ) applied to the amounts of compound adsorbed at the different sampling times indicated an equilibrium time of about 24 h for the three adsorbents (Fig. 4).

The ability of orange peel to remove contaminants such as heavy metals [73] and dyes [74] from aqueous solutions was demonstrated in recent studies; the authors attributed this property to the large surface area per mass unit of the material. Citrus peel can be an excellent adsorbent since it contains high levels of biomolecules (e.g., lignin, cellulose and pectin) and essential oils, which can promote adsorbent-contaminant bonds [75]. Similarly, the use of olive stones as a bioadsorbent for the removal of heavy metals (e.g., Cd (II), Cu (II), Pb (II) and Cr (VI)) from wastewater is well documented [76–79]. Furthermore, the relevant capacity of pistachio shells to adsorb heavy metals, dyes and antibiotics from aqueous media has been recently reported [24,80].

Using the non-linear regression method, experimental data of adsorption kinetics were described with the PFO and PSO equations. Results obtained are shown in Table 4. Values of the correlation coefficient,  $r$ , close to the unit and low values of the sum of squared residuals, SSR, indicate a good correspondence between the experimental data and the model. The results of the kinetic study showed in general a good capacity of the three adsorbents to retain the four molecules from the aqueous medium. At equilibrium, on all materials, the amounts of adsorbed OXY and BPA were much higher than those of adsorbed MET and IMI. This was expected based on the log Kow values of the compounds. Comparing the overall adsorption efficiency of the three adsorbents for all molecules, a similar behaviour was shown by olive stones and pistachio shells, whereas orange peel was less effective (Fig. 4). At equilibrium, the quantities of adsorbed OXY, MET, IMI and BPA on olive stones (the most effective adsorbent) were, respectively, 959, 551, 580 and 968 mg kg<sup>-1</sup> (Table 4). Based on  $r$  and SSR values, the PSO equation was the best fit for all molecules (Table 4). Previous studies showed that very often the best fit of experimental kinetic data of many organic compounds was the PSO model [53,81]. The latter model assumes that the limiting phase of adsorption is the formation of high-energy bonds, such as covalent and hydrogen bonds, between the solute and the adsorbent (chemisorption) or the number of unoccupied adsorption sites on the adsorbent surface, also according to the isotherms, and the slower desorption [54].

### 3.3. Adsorption and desorption isotherms

The adsorption isotherm study describes quantitatively the interaction between an adsorbent and a solute at a given temperature and provide adsorption parameters, such as the adsorption constant and maximum adsorption, which allow to compare the efficiency of different adsorbents for the same solute or the affinity of different solutes for the same adsorbent. To interpret the experimental data, we used the theoretical Freundlich, Langmuir and Henry models. The Freundlich model is based on the hypotheses that (i) the adsorbent has a heterogeneous surface; (ii) the adsorption energy decreases exponentially as the active sites become saturated; and (iii) the solute forms a multilayer coating on the adsorbent; (iv) in diluted systems saturation is never achieved. The Langmuir model is based on the following assumptions: (i) adsorption occurs at specific sites on a homogeneous surface of the adsorbent; (ii) only one molecule of solute binds to each site; (iii) the adsorption energy involved is equivalent for all sites; (iv) there is no chemical interaction between adjacent adsorbed molecules; (v) at equilibrium, the solute molecules form a monolayer on the surface of the adsorbent. The Henry model describes a linear distribution of the solute between the adsorbent and the solution.

Based on the values of  $r$  and SSR obtained applying the theoretical models to the experimental data, the adsorption of all compounds onto the three adsorbents was best described by the Freundlich model, although the other models were often adequate (Table 5). Fig. 5 shows the experimental isotherm data and the plots of the Freundlich model, while Table 5 refers the adsorption

**Table 5**  
Adsorption parameters obtained for OXY, MET, IMI, BPA onto the three adsorbents.

Compound	Henry			Freundlich				Langmuir			
	$r$	SSR	$K_d^a$ ads	$r$	SSR	$K_F$ ads	$1/n$ ads	$r$	SSR	$b^a$	$K_L^b$
Orange peels											
OXY	0.999	178	267.7	0.999	135	270.25	0.97	0.999	133	9407	0.03
MET	0.999	266	192.25	0.999	157	187.61	1.06	0.998	279	6995	0.002
IMI	0.999	96	165.37	0.999	23	168.91	0.95	0.999	18	3158	0.05
BPA	0.999	43	228.20	0.999	25	226.44	1.02	0.999	60	3347	0.006
Olive stones											
OXY	0.992	2129	668.19	0.999	485	699.04	0.76	0.998	1199	2428	0.42
MET	0.999	177	318.43	0.999	174	319.12	0.99	0.999	188	45682	0.007
IMI	0.997	2430	346.30	0.999	572	361.55	0.85	0.996	1225	2977	0.14
BPA	0.991	23950	678.81	0.999	977	711.35	0.74	0.998	1559	20309	0.46
Pistachio shells											
OXY	0.994	13476	605.14	0.999	105	632.97	0.78	0.999	1408	2548.4	0.11
MET	0.999	81	317.26	0.999	81	317.44	1	0.999	97.07	32479	0.1
IMI	0.999	114	297.15	0.999	105	295.98	1.01	0.999	138	27956	0.11
BPA	0.994	11818	568.66	0.999	511	595.79	0.79	0.999	213.6	2431	0.34

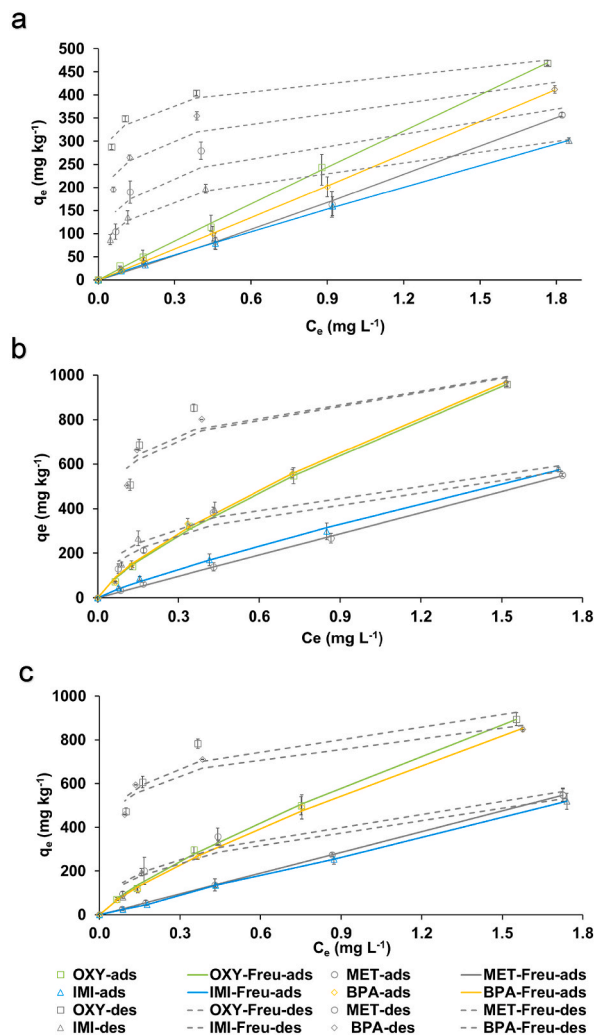


Fig. 5. Experimental data and Freundlich model fit of adsorption/desorption isotherms of OXY, MET, IMI and BPA onto orange peels (a), olive stones (b), and pistachio shells (c). Standard error is reported as vertical bar on each point ( $n = 3$ ).

**Table 6**  
Desorption parameters obtained for OXY, MET, IMI, BPA onto the three adsorbents.

Compound	Henry			Freundlich				Langmuir			
	r	SSR	$K_d$ des <sup>a</sup>	r	SSR	$K_F$ des	1/n des	r	SSR	$b^b$	$K_L^b$
Orange peels											
OXY	0.745	261026	315.58	0.979	723	443.31	0.12	0.980	71	460.87	30.31
MET	0.844	72461	227.06	0.945	3569	313.91	0.28	0.993	442	388.05	6.55
IMI	0.880	34972	182.74	0.996	175	251.26	0.30	0.977	1316	311.96	6.12
BPA	0.787	153686	271.90	0.954	2338	382.80	0.18	0.999	53	425.57	13.80
Olive stones											
OXY	0.795	873362	778.95	0.885	24336	917.77	0.18	0.959	8847	1045.4	10.08
MET	0.907	90534	363.71	0.976	4680	457.54	0.39	0.997	286	658.23	3.06
IMI	0.896	115396	387.03	0.977	4356	487.74	0.36	0.933	1260	663.04	3.78
BPA	0.812	774711	777.53	0.948	11373	909.89	0.20	0.982	4119	1026.2	10.22
Pistachio shells											
OXY	0.800	720507	705.34	0.933	12937	849.81	0.20	0.996	822	963.11	10.35
MET	0.925	69006	357.76	0.974	5633	442.28	0.45	0.998	529	688.36	2.35
IMI	0.926	60156	333.85	0.972	5588	414.81	0.45	0.993	1275	649.03	2.33
BPA	0.795	659112	651.79	0.953	7339	797.96	0.18	0.985	2413	881.84	12.76

<sup>a</sup> ( $\text{mg kg}^{-1}$ ).

<sup>b</sup> ( $\text{L mg}^{-1}$ ).

parameters calculated by interpreting the data at equilibrium with the Freundlich, Langmuir and Henry models. The Freundlich model interpreted very well the adsorption isotherm data of a number of contaminants on various untreated organic waste [51]. Based on  $K_{F ads}$  values, the sorption efficiency of the adsorbents for all compounds followed the order: olive stones > pistachio shells > orange peel (Table 5).

The desorption study describes quantitatively the release of a compound from an adsorbent into the aqueous phase. Experimental desorption data and theoretical curves obtained by applying the Freundlich model are shown in Fig. 5, while Freundlich ( $K_{F des}$  and  $1/n_{des}$ ), Langmuir ( $K_{L des}$  and  $b$ ) and Henry ( $K_{d des}$ ) desorption parameters are shown in Table 6. Desorption of each molecule from any adsorbent was generally slower and incomplete, indicating the occurrence of a hysteresis process. Also in the case of desorption, the Freundlich model was the best fit for all compounds. The highest  $K_{F des}$  values were recorded for olive stones, which indicates that in general the higher the adsorption capacity of an adsorbent the lower the release of the compound.

To the best of our knowledge, this is the first work that examined orange peel, olive stones and pistachio shells for the removal of the four compounds; therefore, a comparison between our results and those of previous studies is not possible. Wu et al. [82] studied the adsorption of OXY on a peanut shells biochar and reported a  $K_{F ads}$  value that was comparable to that found in this study for olive stones. Using a straw-derived adsorbent to retain MET, Cara et al. [83] report a  $K_{F ads}$  value lower than that found in our work for any adsorbent. The removal of IMI by biocomposites of polypyrrol, polyaniline, sodium alginate and peanut shells reported by Ishtiaq et al. [84] was lower than that observed here for the less efficient orange peel. In a recent study by Loffredo et al. [85], the ability of a digestate from agricultural waste to remove MET and BPA from water appeared lower ( $K_F$  values 1.9 and 1.8 times lower, respectively) than that of orange peel. Moussavi and Khosravi [86] studied the adsorption of methylene blue on pistachio shells and reported a  $K_F$  value of  $112.3 \text{ mg kg}^{-1}$ , which is much lower than those found in this study for any pollutant considered. Cobas et al. [87] studied the adsorption of IMI on chestnut shells and obtained a  $K_F$  value that was comparable to those found for the same compound on the three adsorbents examined here. Delgado-Moreno et al. [88] studied the adsorption of OXY and IMI on different biomixtures, among which vermicompost, whose adsorption capacity is well recognized and reported sorption constants similar to those found in this study.

#### 4. Conclusions

Orange peel, olive stones and pistachio shells, due to their large surface area and porosity, the abundance of reactive functional groups and their elemental composition, can behave as bioadsorbents of organic pollutants, especially highly hydrophobic ones. This study quantified the ability of these wastes to remove the pesticides OXY, MET and IMI, and the xenoestrogen BPA from the aqueous medium. The study of adsorption kinetics and the application of kinetic models to experimental data demonstrated that adsorption occurred predominantly as chemisorption, and that the steady state was reached in a relatively short time on all adsorbents. The values of adsorption constants obtained from sorption isotherms and data modeling using the theoretical models of Henry, Freundlich and Langmuir indicated that the high efficiency of the three adsorbents, especially olive stones, in removing the compounds, especially the most hydrophobic OXY and BPA. Desorption of all molecules was slower than adsorption and incomplete (hysteresis) suggesting a persistent ability of the materials to retain the molecules, which is important in remediation applications. Although this study requires further investigation, the overall results obtained demonstrated that unprocessed, low-cost and widely available agro-industrial byproducts can be usefully recycled for the removal of organic contaminants, confirming once again that waste could become a resource. Finally, these materials incorporated into the soil, in addition to representing a useful enrichment of organic matter and plant nutrients, can immobilize contaminants, thus reducing the risks of contamination of food products and the transfer of contaminants into the human and animal food chain.

#### CRedit authorship contribution statement

**Nicola Colatorti:** Writing – original draft, Investigation, Formal analysis, Data curation, Conceptualization. **Carlo Porfido:** Writing – original draft, Investigation, Formal analysis, Data curation. **Daniilo Vona:** Writing – original draft, Investigation, Formal analysis, Data curation. **Giorgio Mazziotta:** Investigation, Formal analysis. **Elisabetta Loffredo:** Writing – review & editing, Supervision, Methodology, Conceptualization.

#### Consent to participate

This article does not contain any studies with human participants or animals performed by any of the authors.

#### Consent to publish

The permission for the usage of the figures and other contents got permission for its reuse in this manuscript.

#### Data availability

The authors declare that the data supporting the findings of this study are available within the paper and any raw data files needed can be asked upon reasonable request.

## Ethical approval

This article does not contain any studies with human participants or animals performed by any of the authors.

## Funding

This study was carried out within the Agritech National Research Center and received funding from the European Union Next-GenerationEU (PIANO NAZIONALE DI RIPRESA E RESILIENZA (PNRR) – MISSIONE 4 COMPONENTE 2, INVESTIMENTO 1.4 – D.D. 1032 17/06/2022, CN00000022). This manuscript reflects only the authors' views and opinions, neither the European Union nor the European Commission can be considered responsible for them. The study was also partly financed by University of Bari Aldo Moro.

## Declaration of competing interest

The authors declare the following financial interests/personal relationships which may be considered as potential competing interests: Nicola Colatorti reports financial support was provided by Agritech National Research Center. If there are other authors, they declare that they have no known competing financial interests or personal relationships that could have appeared to influence the work reported in this paper.

## Acknowledgments

The authors thank the cooperative 'Il Sannicandrese', Sannicandro di Bari, Italy, for providing the olive stones sample used in this study.

## References

- [1] European Directive (E.D.) 2009/128/CE, Off. J. Eur. Union L 309/71 (2009) [eur-lex.europa.eu/legalcontent/EN/TXT/PDF/?uri=CELEX:32009L0128](http://eur-lex.europa.eu/legalcontent/EN/TXT/PDF/?uri=CELEX:32009L0128). (Accessed 19 April 2024).
- [2] C. Mottes, M. Lesueur-Jannoyer, M. Le Bail, E. Malezieux, Pesticide transfer models in crop and watershed systems, a review. *Agronomy for Sustainable Development* 34 (2014) 229–250, <https://doi.org/10.1007/s13593-013-0176-3>.
- [3] C. Gentil, P. Fantke, C. Mottes, C. Basset-Mens, Challenges and ways forward in pesticide emission and toxicity characterization modeling for tropical conditions, *Int. J. Life Cycle Assess.* 25 (2020) 1290–1306, <https://doi.org/10.1007/s11367-019-01685-9>.
- [4] J. Regueiro, O. López-Fernández, R. Rial-Otero, B. Cancho-Grande, J. Simal-Gándara, A review on the fermentation of foods and the residues of pesticides-biotransformation of pesticides and effects on fermentation and food quality, *Crit. Rev. Food Sci. Nutr.* 55 (2015) 839–863, <https://doi.org/10.1080/10408398.2012.677872>.
- [5] C. Carnimeo, A. Gelsomino, G. Cirrottola, M.R. Panuccio, E. Loffredo, Compost and vermicompost in cucumber rhizosphere promote plant growth and prevent the entry of anthropogenic organic pollutants, *Sci. Hortic.* 303 (2022) 111250, <https://doi.org/10.1016/j.scienta.2022.111250>.
- [6] J.M. Camadro, M. Matringe, F. Thome, N. Brouillet, R. Mornet, P. Labbe, Photoaffinity labeling of protoporphyrinogen oxidase, the molecular target of diphenylether-type herbicides, *Eur. J. Biochem.* 229 (1995) 669–674, <https://doi.org/10.1111/j.1432-1033.1995.0669j.x>.
- [7] M. Mehdizadeh, E. Izadi-Darbandi, M.T.N.P. Yazdi, M. Rastgoo, B. Malaek-Nikouei, H. Nassirli, Impacts of different organic amendments on soil degradation and phytotoxicity of metribuzin, *Int. J. Recycl. Org. Waste Agric.* 8 (2019) 113–121, <https://doi.org/10.1007/s40093-019-0280-8>.
- [8] USEPA Office of Water Report, Candidate contaminant list regulatory determination support document for metribuzin. [https://www.epa.gov/sites/%20production/files/201409/documents/support\\_cc1\\_metribuzin\\_cc1\\_regdet.pdf](https://www.epa.gov/sites/%20production/files/201409/documents/support_cc1_metribuzin_cc1_regdet.pdf), 2023. (Accessed 24 January 2024).
- [9] A.J. Crossthwaite, A. Bigot, P. Camblin, J. Goodchild, R.J. Lind, R. Slater, P. Maienfisch, The invertebrate pharmacology of insecticides acting at nicotinic acetylcholine receptors, *J. Pestic. Sci.* 42 (3) (2017) 67–83, <https://doi.org/10.1584/jpestics.D17-019>.
- [10] S.M. Ensley, Chapter 40 – Neonicotinoids. *Veterinary Toxicology*, Third Edition, 2018, pp. 521–524, <https://doi.org/10.1016/B978-0-12-811410-0.00040-4>.
- [11] *Endocrine Disruptors List. Substances Identified as Endocrine Disruptors at EU Level. Available online at Substances Identified as Endocrine Disruptors at EU Level | Endocrine Disruptor List, 2023 edlists.org.* (Accessed 19 April 2024).
- [12] L. Chen, D. Li, Y. Huang, W. Zhu, Y. Ding, C. Guo, Preparation of sludge-based hydrochar at different temperatures and adsorption of BPA, *Water Sci. Technol.* 82 (2020) 255–265, <https://doi.org/10.2166/wst.2020.096>.
- [13] A.M. Calafat, X. Ye, L.Y. Wong, J. Reidy, L.L. Needham, Exposure of the U.S. Population to bisphenol A and 4-tertiary-Octylphenol: 2003–2004, *Environ. Health Perspect.* 116 (2008) 39–44, <https://doi.org/10.1289/ehp.10753>.
- [14] S.P. den Braver-Sewradj, R. van Spronsen, E.V.S. Hessel, Substitution of bisphenol A: a review of the carcinogenicity, reproductive toxicity, and endocrine disruption potential of alternative substances, *Crit. Rev. Toxicol.* 50 (2020), <https://doi.org/10.1080/10408444.2019.1701986>.
- [15] M. Grassi, G. Kaykioglu, V. Belgiorio, G. Lofrano, Removal of emerging contaminants from water and wastewater by adsorption process, *Emerging Compounds Removal from Wastewater* (2012) 15–37, [https://doi.org/10.1007/978-94-007-3916-1\\_2](https://doi.org/10.1007/978-94-007-3916-1_2).
- [16] E. Loffredo, Recent advances on innovative materials from biowaste recycling for the removal of environmental estrogens from water and soil, *Materials* 15 (2022) 1894, <https://doi.org/10.3390/ma15051894>.
- [17] M.C. Martí-Calatayud, R. Heßler, S. Schneider, C. Bohner, S. Yüce, M. Wessling, R.F. Sena, G.B. Athayde Júnior, Transients of micropollutant removal from high-strength wastewaters in PAC-assisted MBR and MBR coupled with high-retention membranes, *Separ. Purif. Technol.* 246 (2020) 1383–5866, <https://doi.org/10.1016/j.seppur.2020.116863>.
- [18] S. Liu, X. Tong, S. Liu, D. An, J. Yan, Y. Chen, J. Crittenden, Multi-functional Tannic Acid (TA)-Ferric Complex Coating for Forward Osmosis Membrane with Enhanced Micropollutant Removal and Antifouling Property, vol. 626, 2021 119171, <https://doi.org/10.1016/j.memsci.2021.119171>.
- [19] K.C. Dao, C.C. Yang, K.F. Chen, Y.P. Tsai, Recent trends in removal pharmaceuticals and personal care products by electrochemical oxidation and combined systems, *Water* 12 (2020) 1043, <https://doi.org/10.3390/w12041043>.
- [20] N.E. Paucar, I. Kim, H. Tanaka, C. Sato, Ozone treatment process for the removal of pharmaceuticals and personal care products in wastewater, *The Journal of the International Ozone Association* 41 (2019) 3–16, <https://doi.org/10.1080/01919512.2018.1482456>.
- [21] E. Loffredo, E. Taskin, Adsorptive removal of ascertained and suspected endocrine disruptors from aqueous solution using plant-derived materials, *Environ. Sci. Pollut. Control Ser.* 24 (2017) 19159–19166, <https://doi.org/10.1007/s11356-017-9595-z>.
- [22] H.K. Hansen, F. Arancibia, C. Gutiérrez, Adsorption of copper onto agriculture waste materials, *J. Hazard Mater.* 180 (2010) 442–448, <https://doi.org/10.1016/j.jhazmat.2010.04.050>.
- [23] V. Krstić, T. Urošević, B. Pešovski, A review on adsorbents for treatment of water and wastewaters containing copper ions, *Chem. Eng. Sci.* 192 (2018) 273–287, <https://doi.org/10.1016/j.ces.2018.07.022>.

- [24] B. Kayranli, O. Gok, T. Yilmaz, G. Gok, H. Celebi, I.Y. Seckin, O.C. Mesutoglu, Low-cost organic adsorbent usage for removing Ni<sup>2+</sup> and Pb<sup>2+</sup> from aqueous solution and adsorption mechanisms, *Int. J. Environ. Sci. Technol.* 19 (2022) 3547–3564, <https://doi.org/10.1007/s13762-021-03653-z>.
- [25] E. Loffredo, Y. Scarcia, M. Parlavacqua, Removal of ochratoxin A from liquid media using novel low-cost biosorbents, *Environ. Sci. Pollut. Control Ser.* 27 (2020) 34484–34494, <https://doi.org/10.1007/s11356-020-09544-z>.
- [26] H.M El Refay, A.M. Raslan, A.M.E. Atia, Application of low-cost adsorption technique on organic pollutant dye removal by bio-waste adsorbents, *Egypt. J. Chem.* 65 (2022) 977–991, <https://doi.org/10.21608/ejchem.2022.132441.5847>.
- [27] FAOSTAT, Crops and livestock products: orange. <https://www.fao.org/faostat/en/#data/QCL/visualize>, 2022. (Accessed 19 April 2024).
- [28] J.A. Siles, F. Vargas, M.C. Gutiérrez, A.F. Chica, M.A. Martín, Integral valorisation of waste orange peel using combustion, biomethanisation and co-composting technologies, *Bioresour. Technol.* 211 (2016) 173–182, <https://doi.org/10.1016/j.biortech.2016.03.056>.
- [29] S. Dey, S.R. Basha, G.V. Babu, T. Nagendra, Characteristic and biosorption capacities of orange peels biosorbents for removal of ammonia and nitrate from contaminated water, *Cleaner Materials* 1 (2021) 100001, <https://doi.org/10.1016/j.clema.2021.100001>.
- [30] FAOSTAT, Crops and livestock products: olive. <https://www.fao.org/faostat/en/#data/QCL/visualize>, 2022. (Accessed 19 April 2024).
- [31] F. Sciubba, L. Cronopoulou, D. Pizzichini, V. Lionetti, C. Fontana, R. Aromalo, S. Socciarelli, L. Gambelli, B. Bartolacci, E. Finotti, A. Benedetti, A. Miccheli, U. Neri, C. Palocci, D. Bellincampi, Olive mill wastes: a source of bioactive molecules for plant growth and protection against pathogens, *J. Biol.* 9 (2020) 450, <https://doi.org/10.3390/biology9120450>.
- [32] G. Di Giacomo, P. Romano, Evolution of the olive oil industry along the entire production chain and related waste management, *Department of Industrial and Information Engineering and of Economics (DIIE)* 15 (2022), <https://doi.org/10.3390/en15020465>. Engineering Headquarters of Roio, University of L'Aquila.
- [33] FAOSTAT, Crops and livestock products: pistachio. <https://www.fao.org/faostat/en/#data/QCL/visualize>, 2022. (Accessed 19 April 2024).
- [34] B. Hosseinzai, M.J. Hadianfard, B. Aghabarari, M. García-Rollán, R. Ruiz-Rosas, J.M. Rosas, J. Rodríguez-Mirasol, T. Cordero, Pyrolysis of pistachio shell, orange peel and saffron petals for bioenergy production, *Bioresour. Technol. Rep.* 19 (2022) 101209, <https://doi.org/10.1016/j.biteb.2022.101209>.
- [35] A. Moubarik, N. Grimi, Valorization of olive stone and sugar cane bagasse by-products as biosorbents for the removal of cadmium from aqueous solution, *Food Res. Int.* 73 (2014) 169–175, <https://doi.org/10.1016/j.foodres.2014.07.050>, 2014.
- [36] I. Şentürk, M. Alzein, Adsorptive removal of basic blue 41 using pistachio shell adsorbent - performance in batch and column system, *Sustainable Chemistry and Pharmacy* 16 (2020) 100254, <https://doi.org/10.1016/j.scp.2020.100254>.
- [37] G. Rodríguez, A. Lama, R. Rodríguez, A. Jiménez, J. Fernández-Bolaños, Olive stone an attractive source of bioactive and valuable compounds, *Bioresour. Technol.* 99 (2008) 5261–5269, <https://doi.org/10.1016/j.biortech.2007.11.027>, 2008.
- [38] N. Mahato, M. Sinha, K. Sharma, R. Koteswararao, M.H. Cho, Modern extraction and purification techniques for obtaining high purity food-grade bioactive compounds and value-added co-products from citrus wastes, *Foods* 8 (2019) 523, <https://doi.org/10.3390/foods8110523>.
- [39] R.M. Reda, N.M. El Gaafary, A.A. Rashwan, F. Mahsoub, N. El -Gazzar, Evaluation of olive stone biochar as valuable and inexpensive agro- waste adsorbent for the adsorption and removal of inorganic mercury from Nile tilapia aquaculture systems, *Aquacult. Res.* 53 (2022) 1676–1692, <https://doi.org/10.1111/are.15699>.
- [40] M.P. Schmidt, D.J. Ashworth, N. Celis, A.M. Ibekwe, Optimizing date palm leaf and pistachio shell biochar properties for antibiotic adsorption by varying pyrolysis temperature, *Bioresour. Technol. Rep.* 21 (2023), <https://doi.org/10.1016/j.biteb.2022.101325>, 2023.
- [41] G. Reuland, S. Sleutel, H. Li, H. Dekker, I. Sijm, E. Meers, Quantifying CO<sub>2</sub> emissions and carbon sequestration from digestate-amended soil using natural <sup>13</sup>C abundance as a tracer, *Agronomy* 13 (2023) 2501, <https://doi.org/10.3390/agronomy13102501>.
- [42] B. Giannetta, C. Plaza, M. Cassetta, G. Mariotto, I. Benavente-Ferraces, J.C. García-Gilas, M. Panettieri, C. Zaccone, The effects of biochar on soil organic matter pools are not influenced by climate change, *J. Environ. Manag.* 341 (2023) 118092, <https://doi.org/10.1016/j.jenvman.2023.118092>.
- [43] R. Paradelo, K. Al-Zawahreh, M.T. Barral, Utilization of composts for adsorption of methylene blue from aqueous solutions: kinetics and equilibrium studies, *Materials* 13 (2020) 2179, <https://doi.org/10.3390/ma13092179>.
- [44] E. Loffredo, C. Carnimeo, V. D'Orazio, N. Colatorti, Sorption and release of the pesticides oxyfluorfen and boscalid in digestate from olive pomace and in digestate-amended soil, *J. Soils Sediments* 24 (2024) 1489–1506, <https://doi.org/10.1007/s11368-024-03748-3>.
- [45] T.G. Ambaye, M. Vaccari, E.D. van Hullebusch, A. Amrane, S. Rtimi, Mechanisms and adsorption capacities of biochar for the removal of organic and inorganic pollutants from industrial wastewater, *Int. J. Environ. Sci. Technol.* 18 (2021) 3273–3294, <https://doi.org/10.1007/s13762-020-03060-w>.
- [46] M. Ahmad, A.U. Rajapaksha, J.E. Lim, M. Zhang, N. Bolan, D. Mohan, M. Vithanage, S.S. Lee, Y.S. Ok, Biochar as a sorbent for contaminant management in soil and water: a review, *Chemosphere* 99 (2014) 19–33, <https://doi.org/10.1016/j.chemosphere.2013.10.071>.
- [47] M. Jeguirim, M. Belhachemi, L. Limousy, S. Bennici, Adsorption/reduction of nitrogen dioxide on activated carbons: textural properties versus surface chemistry – a review, *Chem. Eng. J.* 347 (2018) 493–504, <https://doi.org/10.1016/j.cej.2018.04.063>.
- [48] S. Safarian, Climate impact comparison of biomass combustion and pyrolysis with different applications for biochar based on LCA, *Energies* 16 (2023) 5541, <https://doi.org/10.3390/en16145541>.
- [49] J.O. Eniola, B. Siziirici, Y. Fseha, J.F. Shaheen, A.M. Aboulella, Application of conventional and emerging low-cost adsorbents as sustainable materials for removal of contaminants from water, *Environ. Sci. Pollut. Control Ser.* 30 (2023) 88245–88271, <https://doi.org/10.1007/s11356-023-28399-8>.
- [50] S. Patel, Potential of fruit and vegetable wastes as novel biosorbents: summarizing the recent studies, *Rev. Environ. Sci. Biotechnol.* 11 (2012) 365–380, <https://doi.org/10.1007/s11157-012-9297-4>.
- [51] M.A. Frezzini, L. Massimi, M.L. Astolfi, S. Canepari, A. Giuliano, Food waste materials as low-cost adsorbents for the removal of volatile organic compounds from wastewater, *Materials* 12 (24) (2019) 4242, <https://doi.org/10.3390/ma12244242>.
- [52] E.V. Shamrikova, E.V. Vanchikova, E.V. Kyzurova, E.V. Zhangurov Ev, Methods for measuring organic carbon content in carbonate-containing soils: a review, *Eurasian Soil Sci.* 57 (2024) 380–394, <https://doi.org/10.1134/S1064229323603104>.
- [53] K.V. Kumar, Linear and non-linear regression analysis for the sorption kinetics of methylene blue onto activated carbon, *J. Hazard Mater.* 137 (2006) 1538–1544, <https://doi.org/10.1016/j.jhazmat.2006.04.036>.
- [54] Y.S. Ho, G. McKay, Pseudo-second order model for sorption processes, *Process Biochem.* 34 (1999) 451–465, [https://doi.org/10.1016/S0032-9592\(98\)00112-5](https://doi.org/10.1016/S0032-9592(98)00112-5).
- [55] N.G. Turan, B. Mesci, Use of pistachio shells as an adsorbent for the removal of zinc(II) ion, *Clean* 39 (2011) 475–481, <https://doi.org/10.1002/clean.201000297>.
- [56] A. Khalfaoui, A. Benalia, Z. Selam, A. Hammoud, K. Derbal, A. Panico, A. Pizzi, Removal of chromium (VI) from water using orange peel as the biosorbent: experimental, modeling, and kinetic studies on adsorption isotherms and chemical structure, *Water* 16 (2024) 742, <https://doi.org/10.3390/w16050742>.
- [57] J.F. García Martín, M. Cuevas, C.H. Feng, et al., Energetic valorisation of olive biomass: olive-tree pruning, olive stones, and pomaces, *Processes* 8 (2020) 511, <https://doi.org/10.3390/pr8050511>.
- [58] P. Balasundar, P. Narayanasamy, S. Senthil, N.A. Al-Dhabi, R. Prithivirajan, R. Shyam, R. Kumar, T. Ramkumar, K. Subrahmanya Bhat, Physico-chemical study of pistachio (*Pistacia vera*) nutshell particles as a bio-filler for eco-friendly composites, *Mater. Res. Express* 6 (2019) 105339, <https://doi.org/10.1088/2053-1591/ab3b9b>.
- [59] Y.H. Celik, R. Yalcin, T. Topkaya, et al., Characterization of hazelnut, pistachio, and apricot kernel shell particles and analysis of their composite properties, *J. Nat. Fibers* 18 (2021) 1054–1068, <https://doi.org/10.1080/15440478.2020.1739593>.
- [60] S. Gained, Exploitation of orange peel for fungal solubilization of rock phosphate by solid state fermentation, *Waste and Biomass Valorization* 8 (2017) 1351–1360, <https://doi.org/10.1007/s12649-016-9682-2>.
- [61] G.H. Davarynejad, M. Zarei Mohamadabad, N.P. Tamas, Identification and quantification of heavy metals concentrations in pistacia, *Not. Sci. Biol.* 5 (2013) 438–444, <https://doi.org/10.15835/nsb549115>.
- [62] G.B. García, M. Calero de Hoces, C. Martínez García, M.T. Cotes Plomino, A. Ronda Galvez, M.A. Martín-Lara, Characterization and modeling of pyrolysis of the two-phase olive mill solid waste, *Fuel Process. Technol.* 126 (2014) 104–111, <https://doi.org/10.1016/j.fuproc.2014.04.020>, 2014.
- [63] C. Nguyen, J.P. Loison, C. Motard, S. Dauguet, Cadmium partitioning between hulls and kernels in three sunflower varieties: consequences for food/feed chain safety, *Environ. Sci. Pollut. Control Ser.* 31 (2024) 1674–1680, <https://doi.org/10.1007/s11356-023-31631-0>.

- [64] I. Hilber, A.C. Bastos, S. Loureiro, et al., The different faces of biochar: contamination risk versus remediation tool, *J. Environ. Eng. Landsc. Manag.* 25 (2017) 86–104, <https://doi.org/10.3846/16486897.2016.1254089>.
- [65] P. McKendry, Energy production from biomass (part 1): overview of biomass, *Bioresour. Technol.* 83 (2022) 37–46, [https://doi.org/10.1016/S0960-8524\(01\)00118-3](https://doi.org/10.1016/S0960-8524(01)00118-3).
- [66] B. Zapata, J. Balmaseda, E. Fregoso-Israel, E. Torres-García, Thermo-kinetics study of orange peel in air, *J. Therm. Anal. Calorim.* 98 (2009) 309–315, <https://doi.org/10.1007/s10973-009-0146-9>.
- [67] D. Blasi, D. Mesto, P. Cotugno, C.D. Calvano, M. Lo Presti, G.M. Farinola, Revealing the effects of the ball milling pretreatment on the ethanosolv fractionation of lignin from walnut and pistachio shells, *Green Chem. Lett. Rev. N. 15* (2022) 893–902, <https://doi.org/10.1080/17518253.2022.2143244>.
- [68] A.H. Ab Rahim, Z. Man, A. Sarwono, W.S. Wan Hamzah Ws, N.M. Yunus, C.D. Wilfred, Extraction and comparative analysis of lignin extract from alkali and ionic liquid pretreatment, *J. Phys. Conf.* 1123 (2018) 012052.
- [69] R. El Hage, N. Brosse, L. Chrusciel, C. Sanchez, P. Sannigrahi, A. Ragauskas, Characterization of milled wood lignin and ethanol organosolv lignin from miscanthus, *Polym. Degrad. Stabil.* 94 (2009) 1632–1638, <https://doi.org/10.1016/j.polymdegradstab.2009.07.007>.
- [70] S.L. Hsu, J. Patel, W. Zhao, Chapter 10 - vibrational spectroscopy of polymers, *Molecular Characterization of Polymers* (2021) 369–407, <https://doi.org/10.1016/B978-0-12-819768-4.00010-5>.
- [71] G. Buscemi, D. Vona, R. Ragni, R. Comparelli, M. Trotta, F. Milano, G.M. Farindola, Polydopamine/ethylenediamine nanoparticles embedding a photosynthetic bacterial reaction center for efficient photocurrent generation, *Advanced Sustainable Systems* 5 (2021) 2000303, <https://doi.org/10.1002/adsu.202000303>.
- [72] M.L. Del Praud-Audelo, I. García Kerdan, L. Escutia-Guadarrama, J.M. Reyna-Gonzalez, J.J. Magana, G. Leyva-Gomez, Nanoremediation: nanomaterials and nanotechnologies for environmental cleanup, *Front. Environ. Sci.* 9 (2021), <https://doi.org/10.3389/fenvs.2021.793765>.
- [73] T.F. Akinhanmi, E.A.O. Ofudje, A.I. Adeogun, P. Aina, I.G. Mayowa, Orange peel as low-cost adsorbent in the elimination of Cd(II) ion: kinetics, isotherm, thermodynamic and optimization evaluations, *Bioresources and Bioprocessing* 7 (2020) 34, <https://doi.org/10.1186/s40643-020-00320-y>.
- [74] M. Ahmed, F. Mashkoo, A. Nasar, Development, characterization, and utilization of magnetized orange peel waste as a novel adsorbent for the confiscation of crystal violet dye from aqueous solution, *Groundwater for Sustainable Development* 10 (2020) 100322, <https://doi.org/10.1016/j.gsd.2019.100322>.
- [75] U. Michael-Igolima, S.J. Abbazia, A.O. Ifelebuegu, E.U. Eyo, Modified orange peel waste as a sustainable material for adsorption of contaminants, *Materials* 16 (2023) 1092, <https://doi.org/10.3390/ma16031092>.
- [76] M.A. Martín-Lara, G. Blázquez, M.C. Trujillo, A. Pérez, M. Calero, New treatment of real electroplating wastewater containing heavy metal ions by adsorption onto olive stone, *J. Clean. Prod.* 81 (2014) 120–129, <https://doi.org/10.1016/j.jclepro.2014.06.036>.
- [77] G. Hodaifa, S.B.D. Alami, J.M. Ochando-Pulido, M.D. Víctor-Ortega, Iron removal from liquid effluents by olive stones on adsorption column: breakthrough curves, *Ecol. Eng.* 73 (2014) 270–275, <https://doi.org/10.1016/j.ecoleng.2014.09.049>.
- [78] M.B. Amar, K. Walha, V. Salvado, Evaluation of olive stones for Cd(II), Cu(II), Pb(II) and Cr(VI) biosorption from aqueous solution: equilibrium and kinetics, *Int. J. Environ. Res.* 14 (2020) 193–204, <https://doi.org/10.1007/s41742-020-00246-5>.
- [79] A. Agarwal, U. Upadhyay, I. Sreedhar, K.L. Anitha, Simulation studies of Cu(II) removal from aqueous solution using olive stone, *Cleaner Materials* 5 (2022) 100128, <https://doi.org/10.1016/j.clema.2022.100128>.
- [80] I.G. Shaikhiev, N.V. Kraysman, S.V. Svergzova, Review of pistachio (pistacia) shell use to remove pollutants from aqua media, *Biointerface Research in Applied Chemistry* 13 (2023), <https://doi.org/10.33263/BRIAC134.389>.
- [81] E.D. Revellame, D.L. Fortela, W. Sharp, R. Hernandez, M.E. Zappi, Adsorption kinetic modeling using pseudo-first order and pseudo-second order rate laws: a review, *Cleaner Engineering and Technology* 1 (2020) 100032, <https://doi.org/10.1016/j.clet.2020.100032>.
- [82] C. Wu, X. Liu, X. Wu, F. Dong, J. Xu, Y. Zheng, Sorption, degradation and bioavailability of oxyfluorfen in biochar-amended soils, *Sci. Total Environ.* 658 (2019) 87–94, <https://doi.org/10.1016/j.scitotenv.2018.12.059>.
- [83] I.G. Cara, L.C. Trincă, A.E. Trofin, A. Cazacu, D. Țopa, C.A. Peptu, G. Jităreanu, Assessment of some straw-derived materials for reducing the leaching potential of metribuzin residues in the soil, *Appl. Surf. Sci.* 358 (2015) 586–594, <https://doi.org/10.1016/j.apsusc.2015.08.141>.
- [84] F. Ishtiaq, H.N. Bhatti, A. Khan, M. Iqbal, A. Kausar A. Polypyrrole, Polyaniline and sodium alginate biocomposites and adsorption-desorption efficiency for imidacloprid insecticide, *Int. J. Biol. Macromol.* 147 (2020) 217–232, <https://doi.org/10.1016/j.ijbiomac.2020.01.022>.
- [85] E. Loffredo, C. Carnimeo, R. Silletti, C. Summo, Use of the solid by-product of anaerobic digestion of biomass to remove anthropogenic organic pollutants with endocrine disruptive activity, *Processes* 9 (2021) 11, <https://doi.org/10.3390/pr9112018>.
- [86] G. Moussavi, R. Khosravi, The removal of cationic dyes from aqueous solutions by adsorption onto pistachio hull waste, *Chem. Eng. Res. Des.* 89 (2011) 2182–2189, <https://doi.org/10.1016/j.cherd.2010.11.024>.
- [87] M. Cobas, J. Mejjide, M.A. Sanromán, M. Pazos, Chestnut shells to mitigate pesticide contamination, *J. Taiwan Inst. Chem. Eng.* 61 (2016) 166–173.
- [88] L. Delgado-Moreno, R. Nogales, E. Romero, Wastes from the olive oil production in sustainable bioremediation systems to prevent pesticides water contamination, *Int. J. Environ. Sci. Technol.* 14 (2017) 2471–2484, <https://doi.org/10.1007/s13762-017-1335-x>.